Universitat Politècnica de Catalunya (UPC)
Universitat Autònoma de Barcelona (UAB)
Universitat de Barcelona (UB)
Institut de Ciències Fotòniques (ICFO)

http://www.photonicsbcn.eu

Master in Photonics

MASTER THESIS WORK

INFRARED IMAGING SPECTROSCOPY OF SKIN CANCER LESIONS

Laura Rey Barroso

Supervised by Prof. Meritxell Vilaseca Ricart, (CD6)

Presented on date 8th September 2016

Registered at

Escola Tècnica Superior d'Enginyeria de Telecomunicació de Barcelona

Infrared Imaging Spectroscopy of Skin Cancer Lesions.

Laura Rey Barroso
Centre for Sensors, Instruments and Systems Development (CD6), Universitat Politècnica de Catalunya (Terrassa - Barcelona, Spain).
E-mail: 100293919@alumnos.uc3m.es

Abstract. Skin cancer is a disease of the twenty-first century since, unfortunately, being tan is associated to be healthy and good looking. UV radiation produces one of the most aggressive kinds of skin cancer: melanoma; once the damage is done there is no other solution that a rapid and effective diagnosis. Clinical examination and biopsies have shown to be slow and costly in many ways, so the possibility of getting a non-invasive optical detection of skin melanomas became a hot topic in biophotonics. In this context, multispectral imaging systems have approached the problem, but none of them worked inside the infrared range. Hence, this work has been proposed as an interesting, long-term project to further investigate about the possibilities of infrared imaging spectroscopy for the early detection of skin cancer through the development of such a system based on an InGaAs camera.

Keywords: skin cancer, multispectral imaging, nevus, melanoma, reflectance.

1. Introduction

Skin cancer is the uncontrolled growth of abnormal skin cells. It occurs when unrepaired DNA damage to skin cells (most often caused by ultraviolet radiation from sunshine or tanning beds) triggers mutations, or genetic defects, that lead the skin cells to multiply rapidly and form malignant tumors.[1]Surprisingly, in the past three decades, more people have had skin cancer than all other cancers combined.[2]

The development of skin cancer or pre-cancer can be identified clinically when a mole, a birthmark, a beauty mark or a brown spot changes its color, increases its size or thickness, and gets an unusual texture or its outline gets irregular. It can also be identified as a spot or sore that itches, hurts, crusts, erodes or bleeds.[1]Each type of cancer has a different presentation, depending on the affected cell type and the stage at which the disease is recognized (Fig 1).

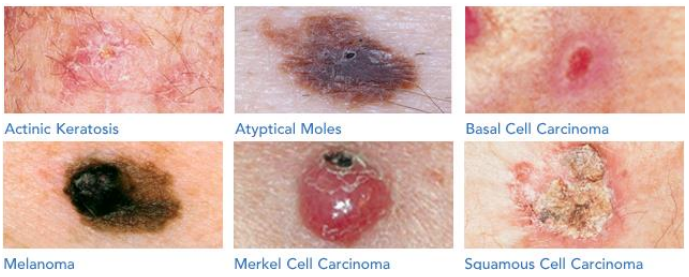

Figure 1. Different types of cancers and pre-cancers.[1]

In the diagnosis process the first contact is visual: a specialist examines the above mentioned changes to determine if these are likely to be a skin cancer.

Unless the clinical exam draws very firm conclusions, a skin biopsy is required, especially if the physician suspects that is a non-superficial kind of skin cancer in order to determine its extent.[3] A biopsy is effective, it determines if there are cancerous cells on a lesion and of which kind are

they. It is a surgical procedure in which specialists are needed to apply anesthesia, make the incision and control the procedure. A specialist in histology is needed as well, for treating the sample and identifying through his/her knowledge and experience what is abnormal under the microscope.

The multiple factors in the chain, make it a long-term process and from the extraction of the tissue until the results are in, it takes two or three weeks.[4]Due to the large number of affected people, there have been many research efforts against skin cancer, in order to better suggest the diagnosis of malignant lesions beyond classical dermoscopy and avoiding unnecessary biopsies. At the CD6, a set of biophotonics-based tools able to measure quantitatively and noninvasively the changing characteristics of melanomas have been developed in the context of the European Project DIAGNOPTICS "Diagnosis of skin cancer using optics" (ICT PSP seventh call for proposals 2013): an interferometry-based system to measure the profile of the lesions (its 3D shape) providing information on roughness and potential ulceration; a blood flow analysis system based on self-mixing technology to measure the amount of angiogenesis that suggests the existence of increased cellular activity caused by a potential malign lesion; and a multispectral system (MS) with a CCD camera to measure the reflectance of skin tissue at different illumination wavelengths along the visible and near-infrared range IR (400nm-1000nm).[5]

MS imaging provides a precise quantification of the different colors present in the skin lesion, that are caused by chromophores such as melanin, hemoglobin, water etc., which might differ among skin lesions of different etiologies.[6] With the CD6's handheld MS system, certain bands have been proved to be useful for improving the diagnosis of skin cancer. However, spectral bands in the IR range beyond 1000 nm have not yet been tested.

Accordingly, the main objectives of this work have been proposed in this context to further investigate about the possibilities of MS systems in the detection of skin cancer, for which an IR imaging spectroscopy system with wavelengths at 970, 1050, 1200, 1350, 1450 and 1550 nm, and an InGaAs camera was developed and calibrated. Clinical measurements of real skin lesions with this experimental system were acquired at the CD6 and the Hospital Clínic i Provincial de Barcelona with the supervision of expert physicians. The final goal was the analysis of the benign and malignant lesions' spectral images using a Matlab® software also developed.

2. State of the Art

Imaging techniques have developed very fast and extensively in the past few years, becoming essential for the study of structures, properties and processes in all the fields in science. Non-invasive tissular studies have become especially popular nowadays because they permit the analysis of processes in vivo, without the alteration of the sample under focus, which were not possible to be studied with the imaging techniques in the past.[7]

Spectral imaging technology has been developed towards the non-invasive studies of polymers, inorganic materials, cells and tissues; with the purpose of characterize them.[8]As a consequence, multispectral systems have developed as well. These systems allow the spectral characterization of a sample (reflectance, radiance, transmittance etc.) through several acquisition channels. The number of channels used in MS systems often ranges from four to ten, since thrichromacy is limited on one side and more than ten channels is unnecessary since most of the samples' spectra are smooth enough, on the other. Every MS system has two fixed elements, a source of illumination and a camera which can be CCD or CMOS, depending on the application, and sensitive to a given spectral range (visible, NIR, IR). But the spectral sampling techniques can change depending whether the system is passive or active. Passive systems illuminate with white light and acquire the information coming from each spectral band with filters. On the other hand, active systems directly illuminate the sample with multiplexed illumination, for instance using light-emitting diodes (LEDs); the sample is illuminated with a different spectral band at a time and information is collected for each pixel.[9]

MS can overcome some of the limitations of classical spectroradiometers and spectrophotometers, lowering the costs by eliminating the expensive diffraction elements and permitting the analysis of a surface area and not just single spot spectral measurements.[10] They

started to be found useful for skin cancer detection a few years ago, especially now that optical detection/selection of skin melanomas is a hot topic in biophotonics. MS systems have been able to analyze reliably and non-invasively the presence of chromophores as fingerprints of any pathology. Different research groups have approached the problem of skin cancer detection with different methods and MS prototypes:

2.1. Multispectral analysis of a benign papilloma by Bekina et al.

The University of Latvia together with the Latvian Oncology Center, in between the years 2011 and 2012 analyzed lesions under a MS with four different spectral bands. These ones were meticulously selected to get information from specific structures of the skin: at 450 nm, information about superficial layers of the skin; at 545 nm, information about blood distribution on the skin; at 660 nm, skin tissue several millimeters in depth providing information about melanin and IR light at 940 nm, with information from deeper skin layers. Then they estimated what they called the erythema index, a ratio between the intensities in green light (560 nm), where the hemoglobin absorption is high, and red light (650 nm), where the hemoglobin absorption is low. It was proved that pathological tissues had this index higher that the surrounding skin as a consequence of having higher blood content. The bilirubin peak was also calculated as the ratio between the intensities at 450 nm and 660 nm and also the melanoma/nevus differentiation parameter, which both were found to be low for benign lesions.[11]

2.2. Modification of a traditional dermoscope by Kapsokalyvas et al.

These authors developed a dermoscope able to illuminate the skin with different wavelengths. By processing the acquired images (operating with them) new contrast images were obtained, each one specific for melanin and hemoglobin absorption, and single scattering; at which different structures could be seen. Analysis of such images could identify pathological morphologies.[12]

2.3. Study of 334 lesions with a MS camera from 450 to 950 nm by Kuzmina et al.

They analysed 334 lesions among which there were 16 melanomas. The MS system used in this case was a camera that incorporated halogen lamps around its objective and filtering from 450 to 950 nm with a spectral bandwidth of 15 nm. Every time the wavelength was increased, they observed a ‘fading’ of spectral images for the three kinds of lesions they analyzed, melanomas, nevi and angiomas. Wavelengths more towards the IR range penetrate deeper in the skin, resulting in decreased contrast due to larger light scattering volume. However, in the case of melanomas at 950 nm the contrast was found to be much higher than that for other pigmented lesions (nevi), so indicating to considerably deeper structural damage of skin. Different chromophores distributions were also analyzed and for the case of melanomas, this ones were more uneven. The fact that melanomas damage the skin deeply, proven with a wavelength of 950 could be a hint to explore further on the IR range. Another proposal for a better melanoma detection includes the use of more chromophores (bilirubin, water) and corrections due to wavelength-dependent scattering.[13]

2.4. Automated diagnosis of pigmented lesions by Tomatis et al.

This research group, related to the National Cancer Institute of Milan, used a spectrophotometer with a light source, a concave mirror incorporating a diffraction grating (monochromator) and a bundle of optical fibers coupled to the probe head. The detector was a camera where for each pixel a calibrated reflectance was calculated automatically. 15 different spectral bands where used from 483 to 950 nm. Then a specialized software based on region growing segmented the lesion and its dark spots inside, in order to take a series of lesion descriptors and filter them according to the sensitivity (the fraction of correctly classified melanomas) and specificity (the fraction of correctly classified benign lesions) that they could offer. After having performed the data reduction, factors and variables were inserted as input for setting and testing a neural network classifier.[14]

As stated above, in the framework of the European Project DIAGNOPTICS, a MS system was developed including a CCD camera and LEDs with emission from the visible to the near IR. The system offers a great amount of spectral data through eight different wavelengths.[6]The statistical management of the data and the use of vector machines are now being implemented and tested to seek for different kinds of information with promising results. The aforementioned research groups and many others all agree that there is a difference between melanomas and nevus at its absorption peak of 600 nm; that a greater hemoglobin absorption indicates more angiogenesis; that bilirubin and other chromophores may indicate the presence of a benign lesion; that carcinogenic lesion tend to be multicolored and with chromophores uneven distributed; etc. But few data is known about MS analysis in the near IR and IR ranges. Since these wavelengths deeply penetrate into the tissue, they may release information about how deeper tissues are damaged due to UV radiation, water content etc. Hence, this work has been proposed as an interesting, long-term project to further investigate about the possibilities of IR imaging spectroscopy to improve skin cancer diagnosis.

3. System design and components

3.1. MS system

The device developed integrates a 16-bit depth InGaAs camera (Hamamatsu) with sensitivity from 900 nm to 1600 nm and 320x256 pixels together with an objective lens adapted to focus properly at the surface of the skin. A ring light source of LEDs on a cylinder of Polyvinyl chloride (PVC) was also developed with emission at 970, 1050, 1200, 1350, 1450 and 1550 nm. The tip of the cylinder is a cone with an opening of 2x2 cm and has a tracing paper ring that serves as a diffuser. In order to obtain a uniform field of enough energy to acquire spectral images with reasonable exposure times, four LEDs per wavelength in opposite corners were finally included in the light source, in total twenty-four LEDs were placed on the ring (Fig. 2).

Figure 2. Camera, light ring, PVC case, mechanical design, power supplies and handled IR MS system.

For the manual use of the system, a handle to hold the cylinder was installed together with a little button to start the measurements once the opening is on top of a lesion. Its design was similar to the one of the visible MS system formerly developed in the DIAGNOPTICS project, compact and ergonomic for the physicians to perform the measurements (Fig. 3).

Figure 3. Handheld IR MS system.

A base of PVC was also designed and constructed to hold the MS system when it is not being used. The base incorporates at the bottom two circular openings where two reference calibrated samples are placed. Two different references and two different dark current images were required, in order to perform a preliminary calibration to compute the spectral results afterwards (see 3.3) (Fig. 4). The references used were two grey colors from the X-Rite color checker, called Neutral 5 and Neutral 6.5. Two different references were used in order to resemble the reflectance of both light and dark skin. The dark current images were acquired without placing any sample on the system.

Figure 4. IR MS system base and color checker. The references chosen are highlighted in red.

3.2. Acquisition software

This is a C++ based software with a friendly interface for physicians to acquire the measurements. The software controls de emission of the LEDs as well as the acquisitions of the IR camera and coordinates them to get a sequence of images. The software interface first asks for a calibration every day, before making any measurements. A calibration is a sequence of acquisition of images, one for each reference, at the six different wavelengths and at ten different exposure times taking into account the LED emission level and also the typical reflectance and absorption properties of the skin. In total, 120 calibration images are acquired (Fig. 5).

These calibration images are kept on a folder named as the date of the acquisition with the format 'MMDDAA'. Then a measurement over the actual skin can be done, and the system will make a sequence of 12 acquisitions, at six different wavelengths for the two references. Each one is acquired with a given exposure time, according to a reference average that has to be reached. The interface asks to enter the name of the patient and the number of the lesion, which is kept with all other lesions from the patient on a folder called as the date of the acquisition 'MMDDAA'. Eventually, other 120 dark current images need to be acquired by just making another calibration in dark conditions, to take into account the noise sensed by the camera at the time of calculating the reflectance curve of a pixel area. The software also includes security controls avoiding LEDs to be switched on if the program is not running.[6]

3.3. Image processing software

In this master thesis, a Matlab® based software was developed to process all the images of the lesions acquired with the Borland Builder C++ interface explained above. The software was adapted from an existing program to manage the information from the visible MS system. The program includes a Graphical User Interface (GUI) from which the images of a given lesion can be opened and displayed, and where a given selected spot or area in the images can be selected to calculate its curve of reflectance (Fig. 5).

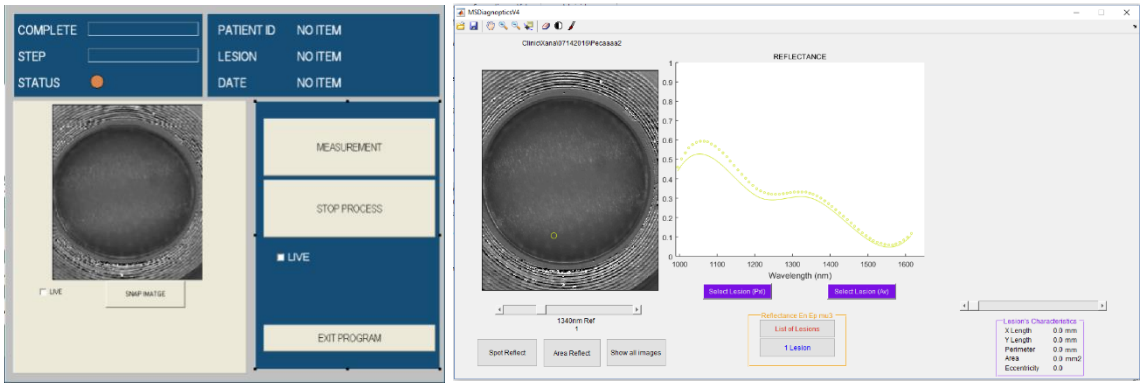

Figure 5. Acquisition software user interface (left) and Matlab GUI (right).

The program has different functions to make internal calibration algorithms and the computation of the reflectance values, in order to finally display the reflectance curve in the Matlab GUI and be able to compare subtle differences between benign and malignant lesions.
In order to calculate the reflectance images of a set of measurement images, the corresponding calibration images from the references and dark current images are selected by the program. It automatically finds the calibration and dark current images inside a folder 'MMDDAA' that matches the one of the selected set of lesion images. Each image from the lesion folder is opened and according to the reference, the wavelength and the digital level at which it was acquired, a specific calibration and a specific dark image are selected and kept inside a 3D cube for the calibration images and a 3D cube for the dark images respectively. Each image from the lesion is also kept on a 3D cube. In this way, all images are sorted properly inside the cubes. Then, the spectral reflectance cube can be calculated by making a pixel by pixel operation with the three cubes. The reflectance at each pixel (i,j) on the cube is calculated as follows:

$$Refl(i,j) = R_{Gi} \cdot \frac{DL(i,j) - DL_0(i,j)}{DL_p(i,j) - DL_0(i,j)} \quad (1)$$

For a given wavelength, this is the spectral reflectance at a single pixel, $Refl(i,j)$. $DL(i,j)$ is the digital level of the raw image, $DL_0(i,j)$ is the digital level of the dark current image, $DL_p(i,j)$ is the digital level of one of the references (Neutral 5 or Neutral 6.5) and R_{Gi} is the calibrated reflectance of the reference, provided by the manufacturer. It was considered helpful to obtain the calibrated reflectance R_{Gi} for both references at the lab, with an integrating sphere and a commercial spectrophotometer for comparison purposes and later validation of the developed MS IR system.

4. System optimization

Specular reflection of the skin was a subject of concern when the first set of lesion images were acquired. The oil, sweat and texture of the skin, and even the position and pressure of the gun on top of the skin, can produce reflections and certain points may appear saturated on the camera.
The perfect situation is one in which the specular reflection is totally removed by a pair of polarizers, but for IR wavelengths these are two heavy pieces of glass that could not be incorporated in this first experimental version of the system.
An important step in the optimization of the MS system was to ensure that these saturated points were not going to affect the final results. In addition, it is known that with a higher optimal average for the skin images, higher exposure times are used by the acquisition software. The higher the exposure times are, the more specular reflection is presented.
So different optimal averages were tried in order to see if there were significant changes. At first, an average of gray 8000 was set as optimal since it is in the middle of the range of the camera (maximum value, 2^{16}), with which images of certain lesions appeared to have quite a lot of glare.

Then, this average was reduced to 6050 and 5050 and the reflection on the lesion images was subtlety reduced at a first glance, but in order to really quantify reflection the number of saturated points present on the images was evaluated with Matlab (Fig. 7).
The code implemented takes a big central area on the pictures and counts the pixels above a certain threshold, which are considered saturated. Different thresholds were tried, from 14500 to 13000 and for each of them, it was proved that lowering the average reduced effectively the number of saturated points. But the number of saturated points was so little in any of the cases that specular reflection was discarded as a problem, and the average of 8000 was kept as optimal.

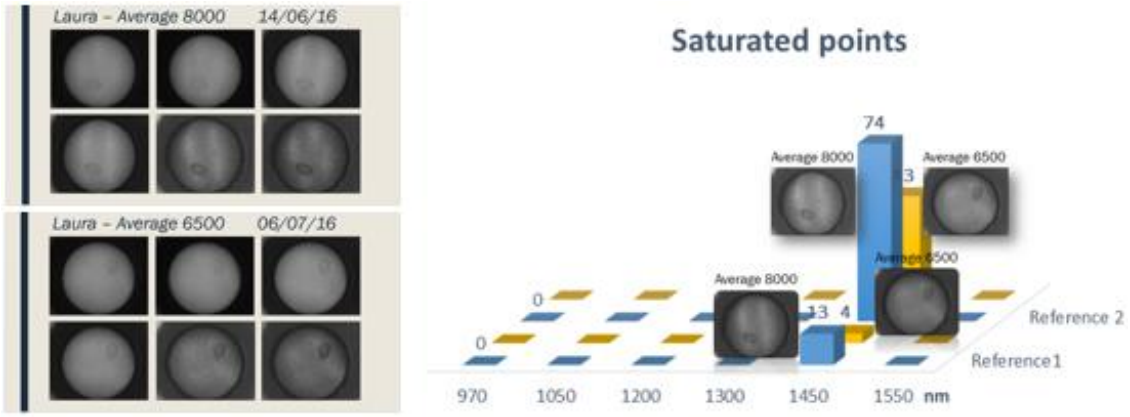

Figure 6. Images with averages of 8000 and 6500 for 970-1550 nm. The difference in saturated points is more noticeable at 1450 nm, but anyhow negligible.

The LEDs firing and image acquisition sequence was also optimized. LEDs' response curve when they are switched on is known to have a sudden peak of power that needs to be avoided,[15] otherwise the images would appear lighter or even saturated. For these reason, a delay from the switch on of the LEDs to the acquisition of the images was introduced. The first delay introduced had a duration of two seconds; it was effective because the averages of the images were the correct ones but the acquisition sequence, especially the one for the calibration was a little slow. Different delays were tried between two seconds and zero seconds. The delay was finally removed because the results show that the peak of the LEDs was not affecting them at all, and hence the sequence of acquisition could be done much faster, in just four or five seconds.
In addition, the repeatability of the measurements was checked. This was done by comparing the gray averages from two different days of calibration and the averages from several calibration measurements acquired sequentially, making sure that the values were maintained. The warming up of the camera and the LEDs may affect the way in which the software finds the correct averages for the calibration images. In either of the cases, the averages did not seem to change considerably. Only on the repetition test, the averages values that the system reached were a little lower each time (Fig. 8). Another issue to be optimized was the reflection of the PVC cone itself. If this material was reflecting the IR wavelengths too much, there was the possibility of coating the inside of the cone with a less reflective paint. First, the averages of the dark current images were calculated and plotted for each wavelength at each exposure time to see if any of them was being particularly reflected by the cone. As it can be seen in the following figure, the gray averages of the dark current images maintained regular values, around a 10% of the maximum value, 2^{16}, which the camera is able to reach. In addition, it can be seen how the averages rise at the same time as the exposure times (and so, the digital levels) increase. The higher the exposure times, the greater amount of noise is produced, as expected (Fig. 8). Then, three circular pieces of PVC were painted with a matt black paint, a shiny black and a silver color respectively. The three of them and a piece of PVC were analyzed under the system and their level of saturation was evaluated. The results indicated that the option that produced less reflections was the PVC itself, hence no paint was applied to the cone.

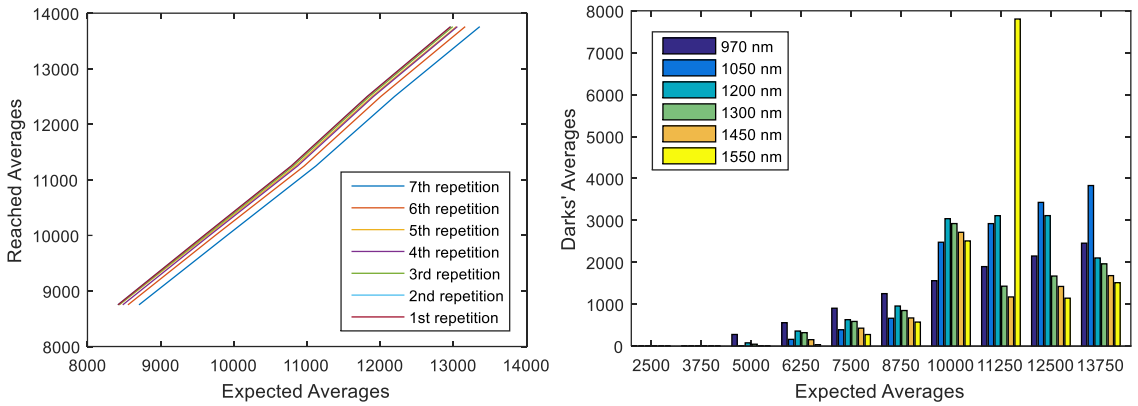

Figure 8. a) Averages values for each repetition at 970 nm. b) Dark images' average gray values.

Finally, once all these optimization was done, some measurements of skin lesions were taken at CD6 and analyzed with the image processing software. Exposure times were checked not to be too high nor too low and the reflectance curve from a point on a lesion was compared with the data obtained by using an integrating sphere of a commercial spectrometer (Instruments Systems Spectro 320) at the lab. The entry permits of the system for the Hospital Clínic de Barcelona were prepared according to the protocols established, such as labeling all the elements of the system. The room in the hospital for conducting the clinical study was visited to install the new IR MS system and learn about the experimental protocol of measurements.

4. Results and conclusions

The last step before entering Hospital Clínic was the validation of the data obtained with this MS system by comparing it to the reflectance curve obtained with the spectrometer. For this purpose, the integrating sphere was used on top of the skin of a voluntary and reflectance data was collected. A measurement over the same skin area was taken with the MS system and the reflectance curve of a point area was obtained with the image processing software. Both curves were compared to be as coincident as possible. The reflectance curves obtained by using both the references Neutral 5 and Neutral 6.5, respectively, were compared among both systems as well.

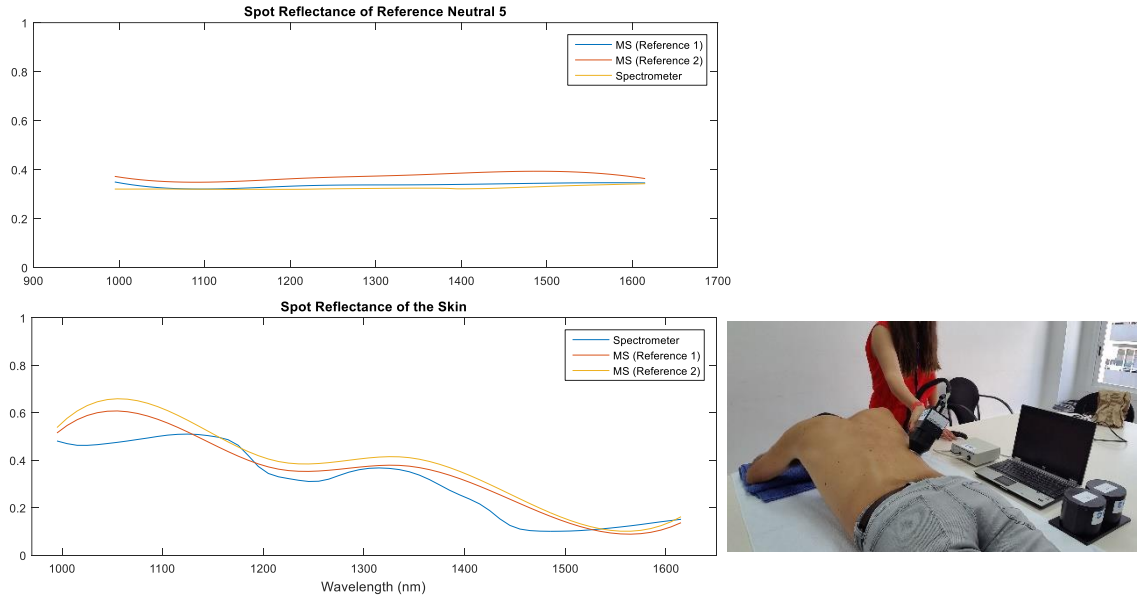

Figure 9. Reflectance curves from the spectrometer and from the IR MS system.

In order to obtain the best coincidence, the acquisition software was made to look for the appropriate exposure times and the dark images were taken once again.
Finally, the system installed at the Dermatology Unit of Hospital Clínic. It was checked to be working properly and left there for physicians to take measurements of patients' lesions that were thought to be malignant. Benign and malignant lesions of different patients are now being acquired. As an example, some of the first reflectance curves that have been obtained are shown in Fig. 9. For the complete analysis among those lesions it is necessary to prepare a full statistical analysis and a machine learning protocol and include a great amount of lesions. All these final steps are now being implemented although they are out of the scope of this work for a matter of time and number of collected lesions.

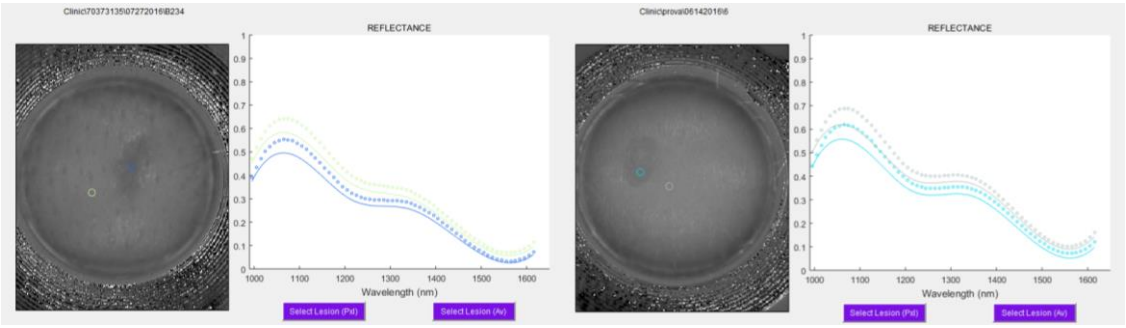

Figure 10. Reflectance curves of a melanoma (left) and a nevus (right). Subtle differences are inherent, but need to be analyzed deeply.

In the future, the same steps for the data analysis of the other modalities will be followed such as those used in the visible range. Different parameters will be analyzed, comparing the healthy surrounding skin with the malignant/benign lesions. For instance, the goodness-of-fit-coefficient (GFC) is used to compare spectral curves based on the inequality of Schwartz[16]:

$$GFC = \frac{\left|\sum_{\lambda=1}^{n}\left(R_\lambda R_{ref,\lambda}\right)\right|}{\sqrt{\left|\sum_{\lambda=1}^{n}(R_\lambda)^2\right|}\sqrt{\left|\sum_{\lambda=1}^{n}\left(R_{ref,\lambda}\right)^2\right|}} \quad (2)$$

Where R_λ is the pixel by pixel reflectance value of the lesion at the λ^{th} wavelength and $R_{ref,\lambda}$ is the average of the skin reflectance that is surrounding the lesion of the patient, obtained from a squared specific area selected manually on the image. Depending to the degree of spectral fitting, from GFC $\geq$ 0.995 to GFC $\geq$ 0.9999, the lesion will be similar to a greater or lesser extent to the healthy skin.

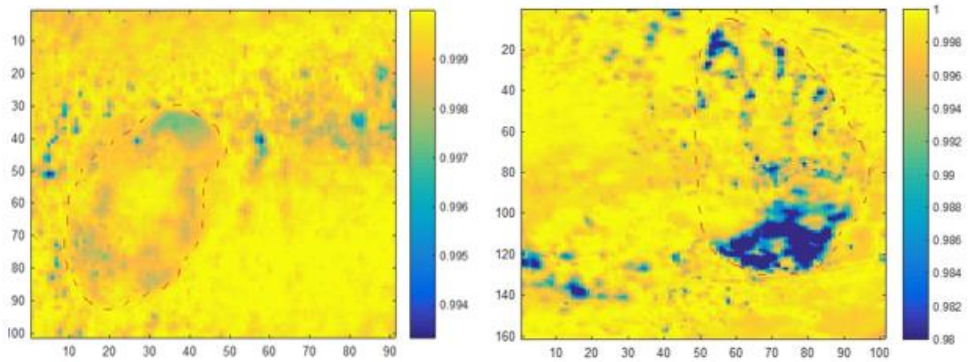

Figure 11. GFC images of a nevus (left) and a melanoma (right). Nevus' GFC values range from GFC>0.995 to 'good spectral fitting' GFC>0.999, the last one associated to a good spectral fitting in the visible, whereas for the melanoma we find lower GFC values inside the lesion (GFC=0.98) which show that the lesion has a very poor spectral fitting to the healthy skin.

Calculating this and other similar parameters for every pixel in the lesion, will permit to get some contrast images and make a deep statistical analysis to quantify the differences among nevi a melanoma, for instance, in terms of the energy, the entropy and the skewness of the digital level histograms at the different spectral bands.

Acknowledgments
This research was supported by the Spanish Ministry of Science and Innovation under the grant DPI2014-56850-R and the European Union.

References

[1] Melia, P. (2016). *The Skin Cancer Foundation - SkinCancer.org*. [online] Skincancer.org. Available at: http://www.skincancer.org/ [Accessed 18 Jul. 2016].
[2] Stern, R. (2010). Prevalence of a History of Skin Cancer in 2007. *Arch Dermatol*, 146(3).
[3] Mayoclinic.org. (2016). *Skin cancer Tests and diagnosis - Mayo Clinic*. [online] Available at: http://www.mayoclinic.org/diseases-conditions/skin-cancer/basics/tests-diagnosis/con-20031606 [Accessed 18 Jul. 2016].
[4] Cancerresearchuk.org. (2014). *Tests for skin cancer | Cancer Research UK*. [online] Available at: http://www.cancerresearchuk.org/about-cancer/type/skin-cancer/diagnosis/tests-for-skin-cancer [Accessed 18 Jul. 2016].
[5] Diagnoptics.eu. (2016). *Project | Diagnoptics*. [online] Available at: http://diagnoptics.eu/project/ [Accessed 19 Jul. 2016].
[6] Delpueyo, X., Vilaseca, M., Royo, S., Ares, M., Sanabria, F., Herrera, J., Burgos, F., Pujol, J., Puig, S., Pellacani, G., Vázquez, J., Solomita, G. and Bosch, T. (2015). Handheld hyperspectral imaging system for the detection of skin cancer. *A: Congress of the International Colour Association. "AIC 2015 Tokyo Proceedings"*, pp.385-390.
[7] Martín Mateos, P., Crespo-Garcia, S., Ruiz-Llata, M., Lopez-Fernandez, J., Jorcano, J., Del Rio, M., Larcher, F. and Acedo, P. (2014). Remote diffuse reflectance spectroscopy sensor for tissue engineering monitoring based on blind signal separation. *BiomedicalOptics Express*, 5(9), p.3231.
[8] Vilaseca, M., Pujol, J., Arjona, M. and de Lasarte, M. (2006). Multispectral system for reflectance reconstruction in the near-infrared region. *Appl. Opt.*, 45(18), p.4241.
[9] Lee, H. (2005). *Introduction to color imaging science*. Cambridge: Cambridge University Press.
[10] Quijano Ruiz, J. (2016). *Quality metrics for spectral estimation*. Master. UniversitatPolitècnica de Catalunya.
[11] Bekina, A., Diebele, I., Rubins, U., Zaharans, J., Derjabo, A. and Spigulis, J. (2012). Multispectral assesment of skin malformations using a modified video-microscope. *The Latvian Journal of Physics and Technical Sciences*, 5.
[12] Kapsokalyvas, D., Bruscino, N., Alfieri, D., de Giorgi, V., Cannarozzo, G., Cicchi, R., Massi, D., Pimpinelli, N. and Pavone, F. (2013). Spectral morphological analysis of skin lesions with a polarization multispectral dermoscope. *Opt. Express*, 21(4), p.4826.
[13] Kuzmina, I., Diebele, I., Jakovels, D., Spigulis, J., Valeine, L., Kapostinsh, J. and Berzina, A. (2011). Towards noncontact skin melanoma selection by multispectral imaging analysis. *J. Biomed. Opt.*, 16(6), p.060502.
[14] Tomatis, S., Carrara, M., Bono, A., Bartoli, C., Lualdi, M., Tragni, G., Colombo, A. and Marchesini, R. (2005). Automated melanoma detection with a novel multispectral imaging system: results of a prospective study. *Physics in Medicine and Biology*, 50(8), pp.1675-1687.
[15] Liu, J. (2009). *Photonic Devices*. California, Los Angeles: Cambridge University Press.
[16] Herrera, J., Vilaseca, M., Burgos, F., Font, L., Sensrrich, R. and Pujol, J. (2014). Imaging from 370 to 1630 nm Using a Novel Multispectral System Based on Light-Emitthing Diodes. *Applied Optics*, 53, pp.373-382.